Original Manuscript

High Performance Polymers

Thermo-oxidative aging and thermal cycling of PETI-340M composites

High Performance Polymers
2021, Vol. 0(0) 1–11

DOI: 10.1177/09540083211033771
journals.sagepub.com/home/hip
SAGE

Xiaochen Li[1], Bo Cheng Jin[1], Thomas K Tsotsis[2] and Steven Nutt[1]

Abstract

Polyimide composites (PETI-340M) were fabricated and subjected to high-temperature aging and thermal cycling to evaluate resistance to degradation. Mechanical-degradation mechanisms and kinetics depended on aging temperature. Aging at 232°C resulted in strength loss due to polymer degradation, while intra-tow cracking was the dominant mechanism during aging at 288°C. Composite panels subjected to thermal-cycling fatigue (−54°C to 232°C) retained mechanical properties without microcracking. However, in regions containing pre-existing fabrication-induced defects (primarily voids), intra-tow microcracks were observed after thermal cycling. Unlike some polyimide composites (PMR-15), oxidative aging effects during thermal cycling were negligible. The thermo-oxidative stability and the retention of mechanical performance after thermal cycling indicates potential for long-term, high-temperature structural applications.

Keywords

Polyimide composites, PETI-340M, thermo-oxidative aging, thermal cycling, compression

Introduction

Oxidative reactions and thermal-cycling fatigue in polyimide composites can cause cracking, embrittlement, and chemical changes, all of which compromise retention of mechanical properties.[1–4] In this work, we explore and report the effects of thermo-oxidative aging and thermal cycling on the mechanical properties and microstructure of PETI-340M (Ube, Tokyo, Japan) composites.

Interest in composite materials for aerospace applications involving harsh environments has driven the development of polyimide composites. Polyimides (PIs) are widely used in high-temperature composite applications because of the high glass-transition temperature (T_g) and thermal stability. However, PMR-15, the long-standing nadic-end–capped polyimide, generally suffers from poor processability, cracking induced by thermal shock, and thermal oxidation. Long exposure to high temperatures can cause damage and loss of strength in such composites. For example, thermal cycling during orbit can cause low-amplitude thermal fatigue and induce damage, including microcracks and delamination.[5,6]

PETI-340M, a phenylethynyl-terminated polyimide (PETI) resin, features relatively low oligomer molecular weight and compatibility with resin transfer molding (RTM) processing. However, the thermo-oxidative stability (TOS) and thermal fatigue resistance have not been investigated or reported. The objective of the present study was to determine the microstructural mechanisms involved in thermo-oxidative degradation and thermal cycling of PETI-340M composites. We investigated the degradation effects on matrix-dominated mechanical properties, including compressive and interlaminar shear strength (ISS). Crack formation during thermal oxidation and thermal cycling were also investigated using light microscopy and micro-computed tomography (micro-CT) (computed tomography). To simulate anticipated service environments, aging was performed at 232°C and 288°C.

Much effort has been devoted to understanding the stability of polyimide composites subjected to thermal-cycling fatigue.[7–12] In conventional polyimide composites, such as PMR-15, as thermal fatigue progresses, the crack density (crack/length of the specimen) increases asymptotically and approaches an equilibrium value, while the coefficient of thermal expansion (CTE) decreases. Microcracks begin as intraply cracks grow to interply cracks as the number of cycles increase, leading ultimately to

[1]M.C. Gill Composites Center, University of Southern California, Los Angeles, CA, USA
[2]The Boeing Company, Long Beach, CA, USA

Corresponding author:
Xiaochen Li, M.C. Gill Composites Center, University of Southern California, 3651 Watt Way, VHE 402, Los Angeles, CA 90089-0001, USA.
Email: xiaochel@usc.edu

delamination. Matrix-dominated mechanical properties, particularly compressive and interlaminar shear strength, are adversely affected by thermal fatigue and thermal aging. Extensional and flexural stiffness are fiber-dominated properties and typically show negligible effects of thermal cycling.

Much of the literature on high-temperature polyimide composites focuses on one formulation—PMR-15. Owens et al. studied the thermal cycling of PMR-15 composites and showed that microcracks initially occurred in the outer plies of laminates until a stress-relieved plateau was reached.[12] Continued cycling resulted in cracking of the inner plies and isothermal aging after thermal cycling produced additional microcracking of inner plies. Tompkins et al. showed that in PMR-15 composites, thermal cycling induced transverse microcracks (TVM) and delamination.[9] The compression and ISS of unidirectional laminates decreased after cycling only when tests were performed at 316°C. However, the ISS of the quasi-isotropic laminate was affected significantly when tested at both room temperature and 316°C. The results indicated the ISS of the quasi-isotropic laminate depended on the density and extent of microstructural damage, while the ISS of the unidirectional laminate depended on both the testing temperature and the damage induced by thermal cycling.[9] Zrida et al. compared two thermal cycles with a common minimum temperature and reported that the highest temperature in the cycle strongly influenced damage development.[7] They also showed that composites were only marginally affected in the high-temperature test, except for panel edges and surface plies that were exposed to air. They also showed that voids in the laminates acted as stress concentrators but also led to larger stress relaxation after crack initiation, which delayed the appearance of new cracks and arrested the growth of existing cracks.

In this study, we investigated the effects of thermo-oxidative aging and thermal-cycling fatigue on matrix-dominated mechanical properties of PETI-340M composites. To better understand the dominant factors affecting mechanical performance, we conducted weight loss measurements, dynamic mechanical analysis (DMA), light microscopy, and micro-CT measurements. The experiments provided a clear understanding of crack initiation, propagation, and the effects on mechanical properties.

This research revealed different aging mechanisms for the two different thermo-oxidative temperatures. Even with a loss in strength, aging at 232°C did not result in aging-induced microcracks, while aging at 288°C produced microcracking. Microcracking induced by thermal cycling was observed only on specimens that possessed fabrication-induced voids or defects. In general, the PETI polyimide showed high thermal stability with retention of mechanical performance.

Experiments

Material preparation and aging condition

A carbon-fiber/polyimide prepreg was selected for this study (PETI-340 M/HTS40 3K 8HS, Ube prepreg using carbon fiber from Teijin Carbon, Tokyo, Japan). The thermoset polyimide matrix system, originally developed for RTM, featured a low processing viscosity. The laminate configuration was quasi-isotropic $[0/+45/-45/90]_{4s}$, and panels were fabricated 2.6-mm thick by 400 mm in length and width. Panels were placed in a vacuum chamber for over 7 days to eliminate moisture before thermal cycling and thermal aging.

Panels prepared for thermal cycling were placed on a mechanically driven sliding tray, and thermal cycling was conducted at −54°C to 232°C, The holding time at each temperature was 15 min. Specimens were removed every 400 cycles to inspect for cracks and for mechanical testing. Thermal-aging specimens were heated in an air-circulated oven at 232°C and 288°C.

All test specimens were water-jet cut from the thermally cycled or thermo-oxidatively aged panels at room temperature and stored in a desiccator at 20°C for over 7 days to remove moisture before mechanical tests were performed.

Dynamic mechanical analysis

The glass-transition temperature, T_g, was measured by DMA (Q800, TA Instruments). A dynamic ramp of 5°C/min was used to heat from 30°C to 400°C, and T_g was determined by both the tan (δ) peak and the transition. Two groups of samples were tested: (1) unaged composites and (2) composites aged at 232°C and 288°C.

Mechanical tests

Compression tests were conducted to determine combined-loading compression (CLC) and open-hole compression (OHC) strength of the unaged composites, aged composites, and thermally cycled composites. Combined-loading compression tests were performed according to ASTM D6641, with a loading rate of 1.3 mm/min, and digital image correlation was used to map displacements (Aramis, Trilion, King of Prussia, PA). Open-hole compression tests were performed using a Boeing-modified testing fixture, a loading rate of 1.3 mm/min, and a test procedure derived from ASTM D6484.

Short-beam shear (SBS) tests were conducted on unaged, thermally cycled, and thermally oxidized composites according to ASTM D2344. Six samples were tested per group using a loading rate of 1 mm/min. Thermo-oxidatively aged composites specimens were tested with a load frame (5567,

INSTRON 5567, Norwood, MA, USA) equipped with an environmental chamber.

Microstructural analysis

Polished sections were prepared and analyzed by light microscopy and micro-CT. To minimize the possibility of additional cracks during machining, more than 1 mm was removed from each edge by grinding. Specimens for light microscopy were polished using sandpaper (grit levels of P240, P400, P600, and P1200) followed by alumina suspension (5 μm and 0.3 μm). Micro-computed tomography scans were performed (XT H 225ST, Nikon, Japan) using Mo-K_α incident radiation with λ = 0.71 A°. Voltage/intensity was set at 60 kV/220 mA to achieve resolution below 4 μm/pixel.

Results and discussion

Weight loss

Figure 1 plots weight loss per unit area for composites as a function of aging time at 232°C and 288°C. The curves show only minor weight loss at 232°C and much more rapid weight loss at 288°C. The curves were produced by nonlinear regression of the experimental data to an allometric power curve (equation (1))

$$\text{Weight loss per unit area} = At^B + C \quad (1)$$

where t = time.

The fitted coefficient and the comparable coefficient for PMR-15 are shown in Table 1. The exponent, B, increases with aging temperature and is influenced significantly by crazing and cracking of the specimen surfaces (B = 1 corresponds to uncracked surfaces).[4]

Comparison of the A and B coefficients for PETI-340M and PMR-15 composites (Table 1) shows that the former composites exhibited greater resistance to thermo-oxidative aging at 288°C. For example, after aging at 288°C for 4000 h, the weight loss per unit area for PMR-15[4] was much greater than the weight loss per unit area for PETI-340M composites (0.644 vs 0.0228 mg/cm^2). The results also show that at 232°C, the coefficient B was 1.035, indicating that the surface of the material was craze-free. However, after aging at 288°C, B increased to 2.068, indicating generation of surface cracks. Aging at 288°C yielded similar B values for PETI-340M and PMR-15 composites (2.068 vs 1.93). However, for PETI-340M composites, coefficients A and C were much less than those of PMR-15 (A: 8.072 × 10^{-10} vs 7.166×$10^{-8,}$ C: 1.177*10^{-4} vs 0.00205), reflected in the relatively low weight-loss rate for PETI-340M composites.

Note that A is a surface-dependent coefficient.[1,4] For the quasi-isotropic PETI-340M laminates, the expression for A is shown in equation (2) where k_1 and k_2 are weight-loss fluxes. S_1 is the area of the un-machined composite surface and corresponds to much higher k_1, especially at the lower aging temperature (T < 288°C).[4] Considering the dimension difference of PETI-340M composites (80 × 80 mm) and PMR-15 composites (25 × 76 mm), weight loss per unit area of PETI-340M composites could be even smaller compared to PMR-15 composites

$$A = S_1k_1 + S_2k_2 \quad (2)$$

where; S_1 = area of composites surface; S_2 = area of cutting with fibers exposed on the surface.

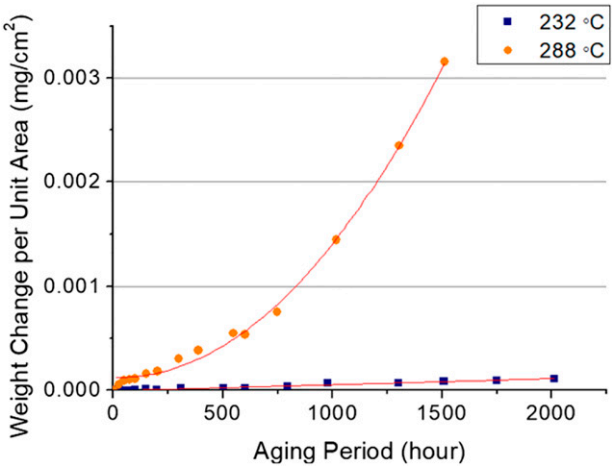

Figure 1. Weight change per unit area for thermo-oxidative aging of PETI-340M composite with nonlinear curve fitting.

Table 1. Coefficients from empirical curve fitting; PETI-340M composites, PMR-15 neat resin, and PMR-15 composites, in milligrams per cubic centimeter.

Material	Aging temperature, °C	A	B	C
PETI-340M composites	232	4.427*10^{-8}	1.035	−4257*10^{-6}
	288	8.072*10^{-10}	2.068	1.177*10^{-4}
PMR-15 neat resin[4]	288	4.914*10^{-1}	0.98	0.25
PMR-15 composites[4]	288	7.166*10^{-8}	1.93	0.00205

Thermal analysis

A prior report on thermo-oxidative aging of 4-phenylethynyl phthalic anhydride (PEPA)–end–capped polyimide revealed asymmetric broadening of the tan (δ) peak at high aging temperature (316°C), indicating the growth of a thick oxidized layer with more compact packing and wider molecular-weight distribution.[13] This peak-broadening has not been reported for aging of PMR-15. However, similar peak-broadening and shouldering were observed for PETI-340M composites aged at 288°C (indicated by red arrow), although it was not observed after aging at 232°C (Figure 2(a)).

Measured changes in T_g are shown in Table 2 and indicate different aging mechanisms at 232°C and 288°C. T_g was measured using the peak of the tan (δ) curve and by the tangents of G'. Aging at the lower temperature showed a decrease in T_g, a result of softening or relaxation of polymer chains. However, aging at 288°C led to formation of a condensed oxidized phase, and T_g increased, a change that occurred in the early stage of aging (< 25 h). Aging at 288°C for 1000 h caused changes detected by DMA. Because of a shouldering effect, a single T_g could not be identified by the peak of the tan (δ) curve after aging at 288°C. A low-temperature peak in the tan (δ) curve (at ~360°C) originated from the interior of the sample, while a broad peak at > 400°C corresponded to the oxidized layer.[13] Compact packing of the surface layer was attributed to the loss of pendant phenyl groups[14] and the generation of oxidative products. These factors led to stronger intra/intermolecular interactions between the polymer chains. The slight increase in G' (Figure 2(b)) was attributed to the reduction in free-volume and decrease of molecule mobility.[13]

Similar changes in T_g after aging was also reported for PMR-15 composites.[15] PMR-15 composites showed an increase of T_g when the aging temperature was > 260°C, but a *decrease* in T_g when the aging temperature was 204°C. The disparities indicated that when conducting accelerated aging studies for polyimide composites (such as PETI-340M, PMR-15, and TriA X), the aging temperature must be selected appropriately to match the temperature of the anticipated application. Although aging conducted at higher aging temperatures (> 288°C) reduces the time for experiments, such tests may also activate a different aging mechanism compared to that of the service temperature.

Morphology

Polished sections of unaged and thermally aged PETI-340M composites are shown in Figure 3. Fresh composites were void-free and crack-free. Similarly, no crack or voids were

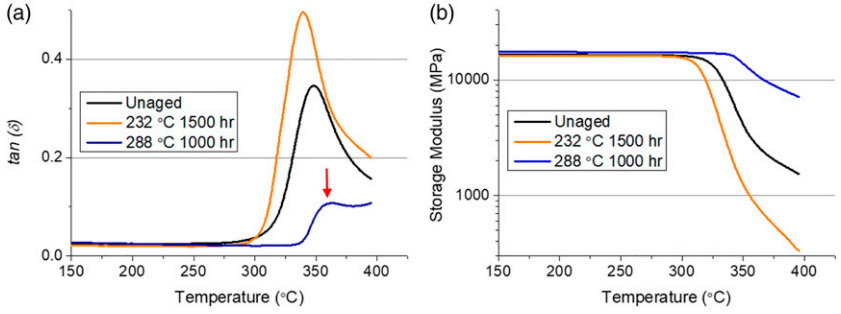

Figure 2. Dynamic mechanical analysis of unaged and thermo-oxidative aged PETI-340M. (a) tan (δ); (b) storage modulus.

Table 2. Change of glass-transition temperature for PETI-340M composites aged at 232°C and 288°C.

	Aging condition	Aging time	T_g (measured by the peak of tan (δ))	T_g (measured by G/ transition)
Material	°C	Hour	°C	°C
PETI-340M composites	Unaged	0	349.89	327.66
	232	25	348.75	334.05
	232	500	352.37	325.86
	232	1000	341.11	305.91
	232	1500	339.38	314.43
	288	25	356.01	332.56
	288	750	—	339.98
	288	1000	—	340.53
	288	1500	—	338.72

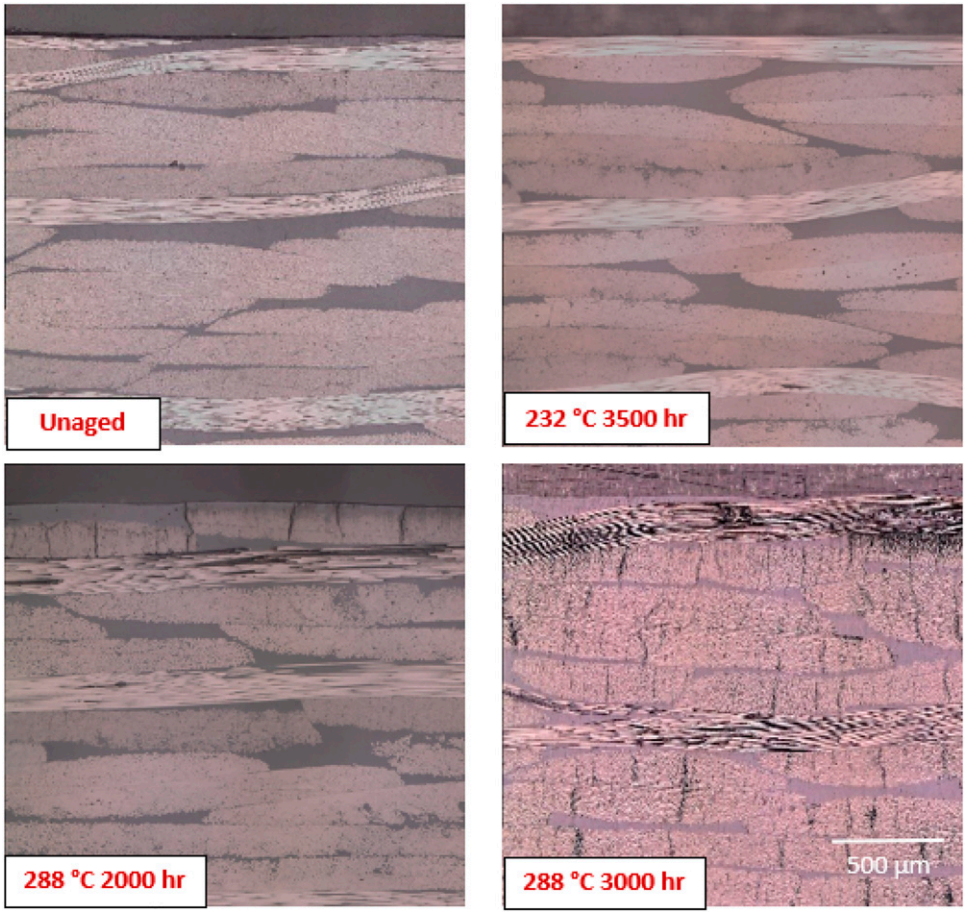

Figure 3. Microscopic image of cross-sections of unaged and aged PETI-340M Composites.

observed for the specimen aged at 232°C for 3500 h, which is consistent with the weight-loss exponent (B = 1.035).

Aging at 288°C for 2000 h produced microcracks in the surface plies of molded composites. Matrix microcracks extended parallel to the fibers within tows, although they were initially intra-tow within surface plies, and later propagated to inner plies. After aging for 3000 h at 288°C, cracks were observed evenly in all plies, and remained intra-tow. Crack generation and propagation from the surface to the inner plies was reflected in the weight-loss exponent coefficient (B = 2.068).

In addition to near-surface cracks, micro-voids started to appear in resin-rich regions after 2000 h aging (Figure 4). The micro-voids formed in surface plies and were evenly distributed in resin-rich regions. The generation of micro-voids was associated with matrix weight loss and shrinkage caused by oxidation reactions. The cracks did not propagate beyond fiber tow boundaries during aging at 288°C for up to 3000 h. The cross-ply architecture of the fabric presented orthogonal tows at tow borders, which acted as crack arrestors. However, delamination occurred when long cracks extended across fiber-rich regions. When aging time exceeded 4000 h, fibers were damaged and often pulled out during polishing, preventing clear sections.

The thermal cycling that occurs in orbit can be considered as low-amplitude thermal fatigue, in which microcracks begin as intraply cracks, grow into interply cracks, and finally cause delamination. In such cases, microcracks arise from thermal cycling, appearing initially in surface plies, until stress relief is achieved.[12] For PMR-15 composites, the crack density approaches an equilibrium value, with the CTE reduced by 40% after 500 cycles between −156°C and 316°C.[16] In the present study, however, a smaller temperature range, −54°C to 232°C, was used for PETI-340M to simulate anticipated service environments.

Two primary types of damage arise during thermal cycling of composites—TVMs and delamination.[9] Transverse microcracks develop when the internal stress exceeds the transverse strength of a lamina due to mismatch between thermomechanical properties of fiber and matrix and between lamina of different fiber orientations. Delamination develops when the thermally cyclic stress generated exceeds the interlaminar strength of the laminate. The stress caused by thermal cycling cannot exceed 50% of the tensile

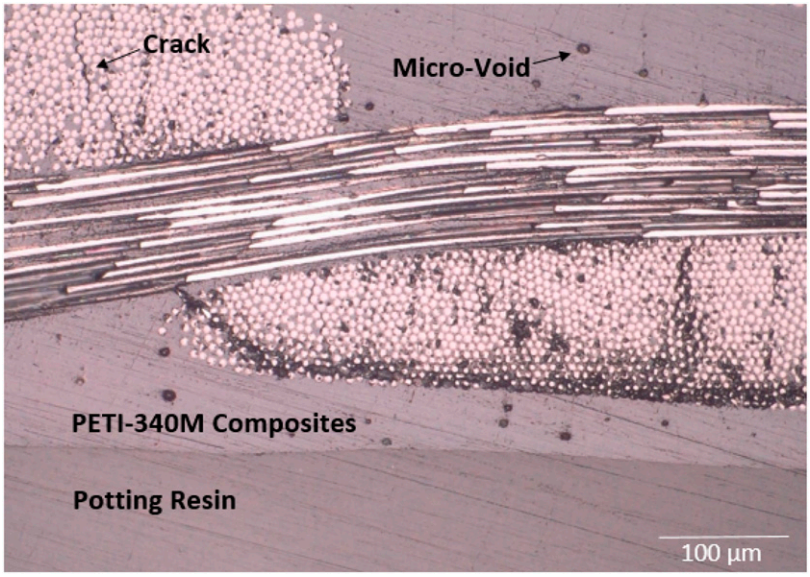

Figure 4. Polished section of PETI-340M composites aged at 288°C for 2500 h.

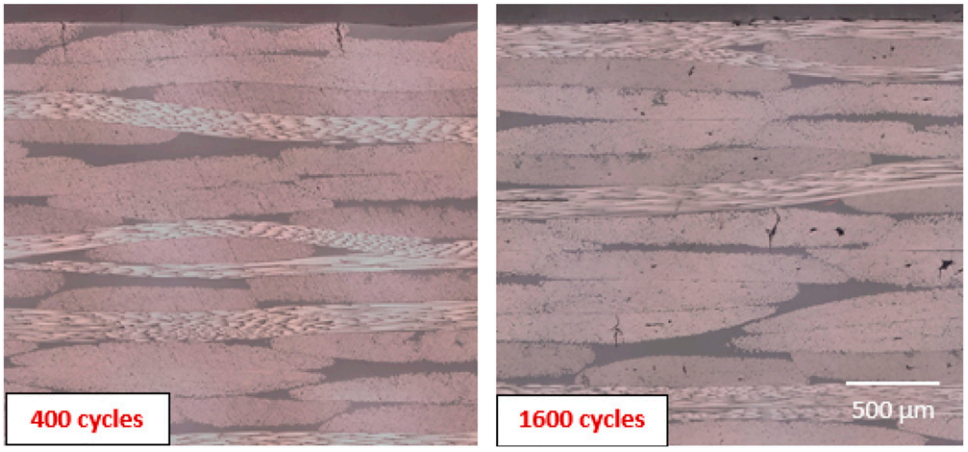

Figure 5. Polished cross-sections of PETI-340M thermal-cycled after 400 cycles and 1600 cycles.

strength of PEPA-terminated polyimide for this thermal-cycling condition.[8] Thus, the polymer matrix is expected to resist microcracking during the thermal cycles used (−54°C to 232°C).

Transverse microcracks were observed after 400, 1600, and 2400 thermal cycles, but not after 800, 1200, and 2000 thermal cycles. PETI-340M composites after 400 and 1600 thermal cycles are shown in Figure 5. Some minor cracks appeared in the surface ply after 400 cycles. However, this type of crack only appeared on one side of the laminate. The appearance of TVM is stochastic and not directly dependent on the number of cycles. Thus, these cracks are attributed to local stress concentrations arising during fabrication or in the sample-mounting press.

A typical microcrack after 1600 thermal cycles is shown in Figure 6. Such microcracks were usually observed within a single fiber tow. However, unlike the intra-tow cracks in thermally aged samples, which did not extend across the tow boundary, cracks induced by thermal cyclic fatigue penetrated the adjoining resin-rich area, as shown in Figure 6. Micro-voids were not observed in resin-rich regions. However, fabrication voids/defects were observed within fiber tows, and these appeared to serve as initiation sites for microcracks during thermal cycling. The second damage mode, delamination, was not observed in PETI-340M composites for this cycling condition.

Based on observations and analysis of microcrack formation during thermal cycling, crack initiation stems from

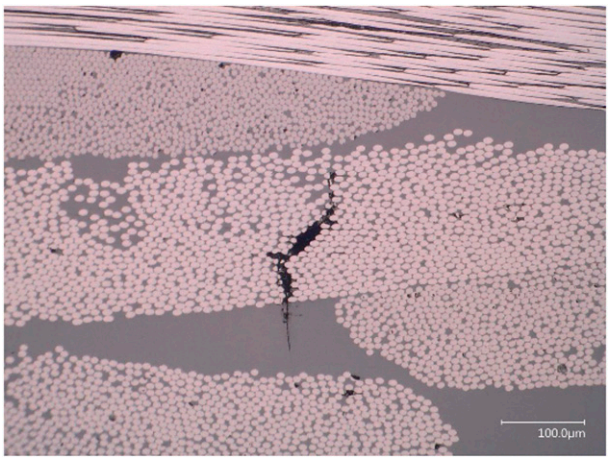

Figure 6. A crack of PETI-340M composites thermal cycled for 1600 cycles.

voids produced during fabrication. However, once a crack initiates, it relieves local stresses, which delays formation of new cracks and arrests the growth of existing cracks.[7] Void-free laminates endure thermal cyclic fatigue without discernible damage in the temperature range chosen (−54°C to 232°C). However, in regions with voids, microcracks will initiate at the defect and propagate during cycling.

PMR-15 composites exhibit a different mechanism for crack-formation, in which microcracks initiate in surface plies, and then propagate to inner plies. Because of the low TOS of PMR-15, thermally induced oxidation is conflated with thermal-cycling fatigue, and thus crack growth follows a pattern similar to thermal aging, which progresses from surface plies to inner plies. In contrast, PETI-340M is thermally stable at the cycling temperature (−54°C to 232°C), and consequently, oxidative aging plays a negligible role during thermal cycling.[7]

Micro-computed tomography images for unaged and thermally cycled PETI-340M composites were analyzed to identify microcracks induced by thermal fatigue. The unaged composites were void-free structures, while after 2400 cycles, cracks appeared as shown in Figure 7 (yellow frames).

Figure 7(a) shows a 3-D image of a transverse section after thermal cycling. In the image, white/gray shading corresponds to low-density regions. The two large gray slabs represent air near the sample, while light gray streaks within the dark core region are internal cracks, which extend primarily in directions parallel to the plies. Figure 7(b) shows an in-plane section. Unlike Figure 7(a), Figure 7(b) clearly reveals the fiber-tow architecture (darker shades represent matrix regions with lower density). The lighter gray regions represent fiber tows, while the dark lines along the fiber tows in the yellow squares are cracks extending parallel to the fibers. Note that in this case, the cracks appear to extend within the same tow, indicating that it may be the same crack.

Cracks appeared in cross-ply (non-crimp) regions throughout the sample thickness, which is consistent with the crack morphology observed by light microscopy. The microcracking is attributed to stress concentrations around fabrication-induced defects, such as incomplete impregnation, which is stochastic in nature. Thus, the observed crack density is independent of the number of thermal cycles, and microcracking appears largely in the middle plies, where incomplete impregnation usually occurs. Voids have two primary effects on thermal-cycling damage. First, they serve as stress concentrators and crack initiation sites, but once initiated, the cracks relax local stresses, and thus delay initiation of new cracks.[13,17] The effect of this type of crack mechanism on mechanical behavior is described in a subsequent section.

Mechanical properties measurements

Thermo-oxidative aging. There have been multiple investigations regarding the TOS of PMR-15 composites, and these studies report two types of thermo-oxidative transformations during thermal aging, including crack initiation at cut edges and surface cracking at molded surfaces.[5] In production, polyimide composites are typically molded into parts, and surface cracks are the dominating factor in mechanical degradation. To better simulate production conditions, after aging, composite edges were trimmed 38 mm and machined to coupons from the middle of plates for mechanical testing.

Compression properties are generally considered to be matrix-dominated, and they play a critical role in service because of failures caused by out-of-plane forces. Both CLC and OHC were performed. Open-hole compression provides a controlled simulation of a natural defect or a fabrication artifact from fasteners. Compression failure can be susceptible to such features, which increase the probability of buckling.

Interlaminar shear strength as a function of aging time was measured by conducting SBS tests (Figure 8). The decline in strength with aging time was attributed to degradation of the matrix and the fiber-matrix interfacial bonding.[9] During SBS tests, specimens also are susceptible to local transverse forces near the loading pins. Thus, detrimental interlaminar shear stresses that develop at local discontinuities can cause local damage and premature failure. In this study, SBS tests showed transverse tensile failure, fiber fracture by buckling, and interply delamination in valid tests.[18]

In Figure 8, both CLC and OHC results showed a decrease in compressive strength after aging at 232 and 288°C. Aging at 288°C for 2500 h caused a 36% decrease in OHC, which matched the decrease in CLC strength (38%). Aging

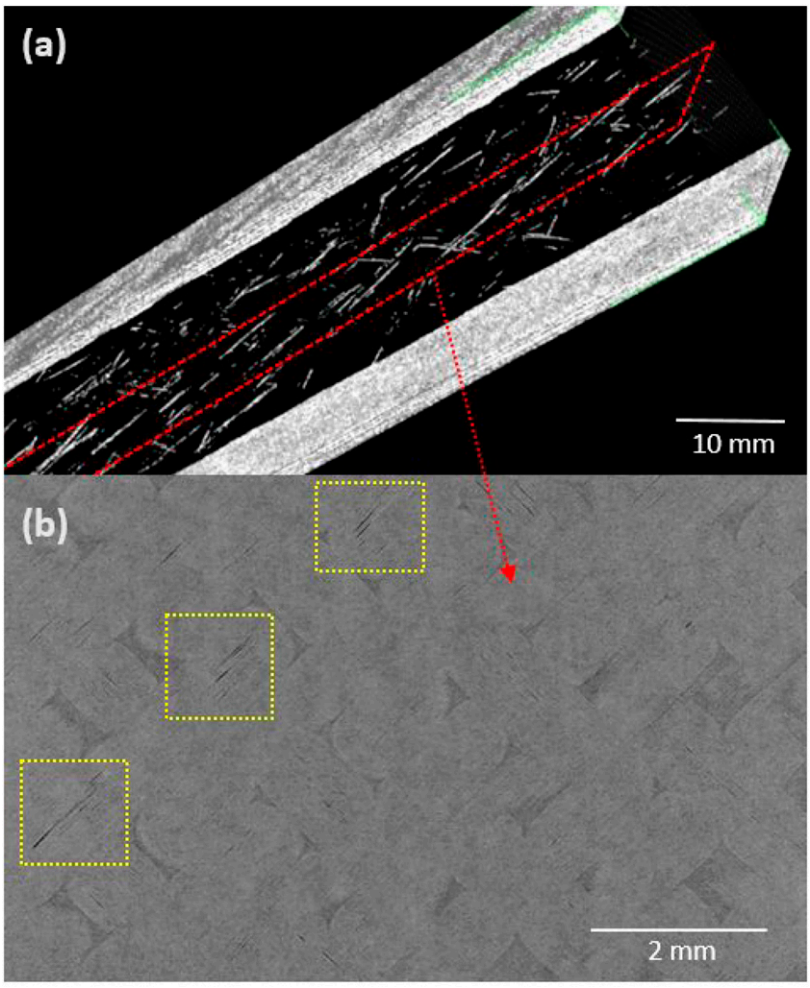

Figure 7. Micro-computed tomography images of specimen after 2400 thermal cycles. (a) 3-D geography; (b) an in-plane cross-section.

at 288°C for 11000 h caused only a 13.7% decrease in OHC strength, and the decrease in CLC strength was slightly more (22.5%). The rate of strength loss with aging time is described by equation (3) below, where S_c can be compressive strength or SBS strength. The fitted m and n are shown in Table 3.

$$S_c = -mt + n \tag{3}$$

The rate of CLC strength loss during aging at 288°C was ~6 times faster than for aging at 232°C. However, the rate of OHC strength loss was ~10 times faster at 288°C, while the rate of SBS strength loss was 8.1 times faster. The difference in the rates of CLC and OHC strength loss was attributed to the fact that the matrix became more rigid and brittle during aging (particularly at 288°C), which increased the crack initiation and propagation rates during hole drilling during OHC sample preparation. The different m values for CLC and SBS strength arose because SBS strength was more sensitive to fiber-matrix interfacial strength, which also decreased during aging.[9]

Chemical changes in the matrix induced by thermo-oxidative aging and crack formation at the surface were the primary factors governing strength loss in polyimide composites. Indeed, the two aging temperatures activated different mechanisms of mechanical degradation. The DMA results showed an *increase* in storage modulus G' after aging at 288°C, but a *decrease* in G' after aging at 232°C. The *decrease* in G' caused by the relaxation, softening, or scission of the polymer chain resulted in the mechanical degradation observed from aging at 232°C. In contrast, the formation and propagation of microcracks from surface plies to inner plies caused the mechanical degradation observed from aging at 288°C. At this temperature, post-curing and oxidation of the matrix, which changed the G' and T_g, was secondary.

In PMR-15 composites, the degradation in compression strength resulting from thermally induced oxidation

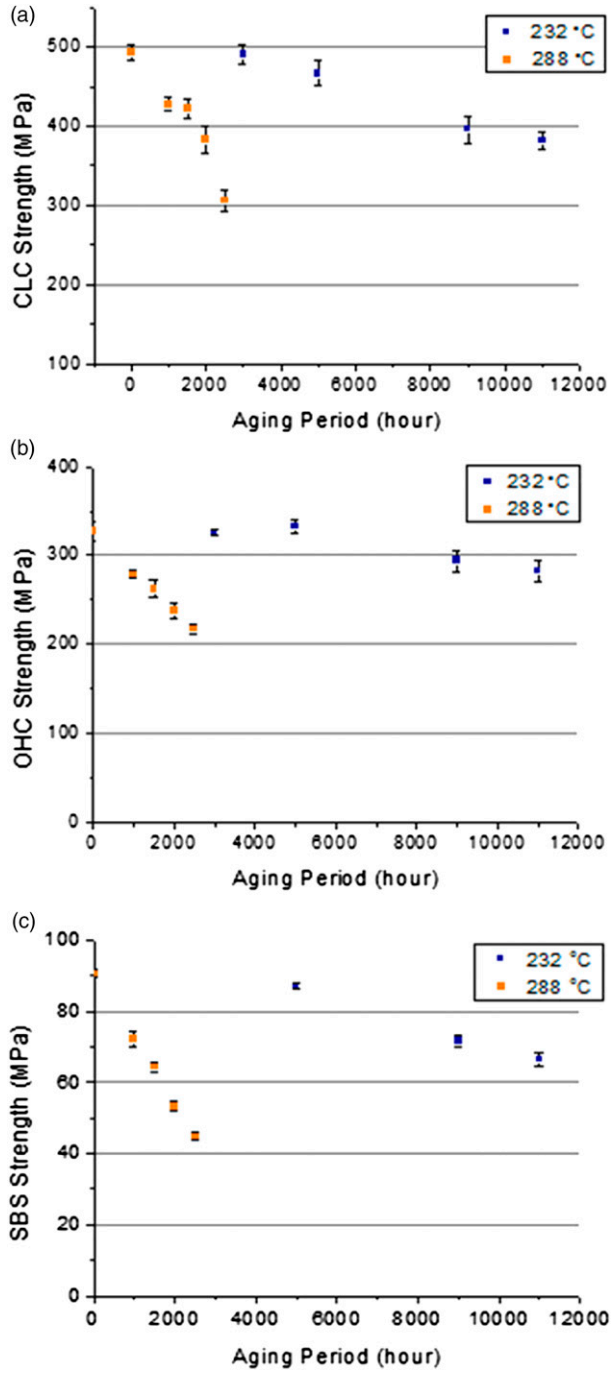

Figure 8. Strength versus aging time for thermally oxidized PETI-340M composites. (a) Combined loading compressive strength; (b) open-hole compressive strength; (c) short-beam shear strength.

occurred by thermal (time-dependent) and oxidative (weight-loss) mechanisms.[5] The same was true for PETI-340M composites studied here, where the rate of weight loss correlated to the retention of compressive strength.[5] However, aging of PMR-15 composites also indicated that the weight-loss behavior was not a reliable indicator of mechanical behavior for aging below 260°C. At higher aging temperatures (> 260°C), the concentration of microcracks in the materials was much greater than for aging at lower temperature (204°C),[5] although the compression strength was similar.

Table 3. Coefficients for the mechanical property degradation of PETI-340M composites aged at 232°C and 288°C.

Mechanical test	Aging temperature, °C	M	*n*
CLC	232	0.0115	509.6
	288	0.0683	502.0
OHC	232	0.0045	337.3
	288	0.0437	325.8
SBS	232	0.00226	92.3
	288	0.0184	90.78

CLC: combined-loading compression; OHC: open-hole compression; SBS: short-beam shear.

Matrix-dominated properties, such as CLC and SBS strength, are most likely to manifest effects of thermal cycling. Before degradation reaches 0-degree plies, which is after significant degradation of the matrix severely affects its ability to transfer load, fiber-dominated properties, such as tensile strength and modulus, show little decrease with thermal cycling, despite initiation of microcracks.[12] Short-beam shear tests were performed at two temperatures (20°C (RT) and 232°C) to assess the effects of test temperature on ISS strength. When tested at RT, the ISS of unidirectional $\{0\}_{20}$ PMR-15 composites was unaffected by thermal cycling despite the fact that cracking and delamination were observed. However, when tested at 316°C, ISS decreased by 15% after 500 cycles.[9]

Strength values as a function of number of thermal cycles is shown in Figure 9. The CLC strength showed a slow increase after 400 thermal cycles (Figure 4(a)), while SBS strength remained largely unaffected at both test temperatures. Microcracking in surface plies caused an initial but slight decrease in CLC strength. However, such cracks relaxed local stresses and also arrested crack growth, limiting crack propagation. Subsequently, post-curing became the dominating factor, causing an increase in CLC strength. However, the SBS strength showed no increase after 400 cycles because ISS is more sensitive to cracking within fiber-rich regions.[13,17]

Unlike PETI-340M composites, PMR-15 composites exhibit microcracking in inner plies during thermal cycling. The cracking reduces the matrix-dominated residual strength at both 20°C and 232°C, although the effect is less pronounced at 232°C, and no change in modulus is observed.[12] In contrast, PETI-340M composites show no change in matrix properties after thermal cycling, and minor cracks are arrested by the cross-ply weave geometry. The

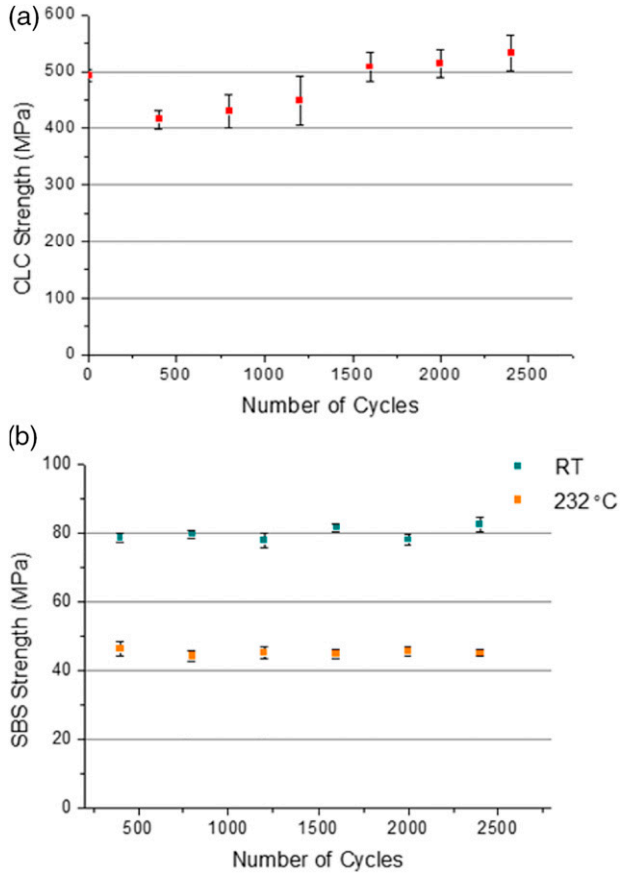

Figure 9. Change of strength of thermal-cycled PETI-340M composites. (a) Combined-loading compressive strength; (b) short-beam shear strength.

retention of strength after thermal cycling can be attributed to the superior thermal stability of the matrix, combined with the woven fiber architecture. In general, PETI-340M composites exhibit greater retention of mechanical properties after aging and thermal cycling compared to PMR-15 composites.

Conclusions

Aging mechanisms were identified for PETI-340M composites aged at two temperatures. Strength loss after aging at 232°C was attributed to matrix weight loss caused by chemical reactions resulting in softening, relaxation, and scission of the polymer chain, with a decrease in T_g. For aging at 288°C, degradation was caused by both matrix oxidation and post-cure, (and an increasing T_g), as well as progressive microcracking. Inter-laminar shear strength was more sensitive to microcracks and delamination in the middle plies compared to unnotched compressive strength. Future investigations of TOS of composites should consider judicious selection of aging temperatures that reflect the intended service temperatures and select mechanical test methods accordingly.

During thermal fatigue, microcracking of PETI-340M composites were initiated at fabrication defects, which concentrated stress locally during thermal cycling despite microcracking; PETI-340M composites retained matrix-dominated properties to a greater degree compared to PMR-15 composites. The superior strength retention was attributed to the greater oxidative stability and the greater tensile strength of the PEPA-terminated polyimide matrix.[8] Void-free PEPA-terminated polyimide composites, PETI-340M, show no cracks or voids after thermal cycling from −54°C to 232°C for 1600 cycles. The superior strength retention of PEPA-terminated polyimide composites indicates potential for long-term structural use in aerospace applications.

Acknowledgments

Material and technical support from the Boeing Company is gratefully acknowledged.

Declaration of conflicting interests

The author(s) declared no potential conflicts of interest with respect to the research, authorship, and/or publication of this article.

Funding

The author(s) received no financial support for the research, authorship, and/or publication of this article.

ORCID iDs

Xiaochen Li https://orcid.org/0000-0001-8789-0293
Steven Nutt https://orcid.org/0000-0001-9877-1978

References

1. Madhukar MS, Bowles KJ and Papadopoulos DS. Thermo-oxidative stability and fiber surface modification effects on the inplane shear properties of graphite PMR-15 composites. *J Compos Mater* 1995; **31**: 596–618.
2. Tandon GP, Pochiraju KV and Schoeppner GA. Thermo-oxidative behavior of high-temperature PMR-15 resin and composites. *Mater Sci Eng A* 2008; **498**(1–2): 150–161.
3. Bowles KJ, Jayne D and Leonhardt TA. Isothermal Aging effect on PMR-15 resin. Washington, DC: NASA Technical Memorandum, 1992, pp. 105648.
4. Bowles KJ and Nowak G. Thermo-oxidative stability studies of celion 6000/PMR-15 unidirectional composites, PMR-15, and celion 6000 fiber. *J Compos Mater* 1988; **22**: 966–985.
5. Bowles KJ, Roberts GD and Kamvouris J. *Long-term isothermal aging effects on carbon fabric-reinforced PMR-15 composites compression strength*, NASA Technical Memorandum, 1995.

6. Meador MAB, Johnston JC, Frimer AA, et al. On the oxidative degradation of nadic end-capped polyimides. 3. Synthesis and characterization of model compounds for end-cap degradation products. *Macromolecules* 1999; **32**: 5532–5538.
7. Zrida H, Fernberg P, Ayadi Z, et al. Microcracking in thermally cycled and aged Carbon fibre/polyimide laminates. *Int J Fatigue* 2017; **94**: 121–130.
8. Zhang Y, Miyauchi M and Nutt S. Effects of thermal cycling on phenylethynyl-terminated PMDA-type asymmetric polyimide composites. *High Perform Polym* 2018; **31**(7): 861–871.
9. Tompkins SS and Williams SL. Effects of thermal cycling on mechanical properties of graphite polyimide. *J Spacecr Rockets* 1984; **21**(3): 274–280.
10. Kim RY, Crasto AS and Schoeppner GA. Dimensional stability of composite in a space thermal environment. *Compos Sci Technol* 2000; **60**: 2601–2608.
11. Berglund LA, Varna J and Yuan J. Transverse cracking and local delamination in $[0_4/90_n]_s$ and $[90_n/04]_s$ carbon fiber/toughned epoxy laminates. *J Reinf Plast Compos* 1992; **11**(6): 643–660.
12. Owens GA and Schofield SE. Thermal cycling and mechanical property assessment of carbon fibre fabric reinforced PMR-15 polyimide laminates. *Compos Sci Technol* 1988; **33**: 177–190.
13. Li X, Miyauchi M, González C, et al. Thermal oxidation of PEPA-terminated polyimide. *High Perform Polym* 2018; **31**(6): 707–718.
14. Miyauchi M, Kazama K-i, Sawaguchi T, et al. Dynamic tensile properties of a novel Kapton-type asymmetric polyimide derived from 2-phenyl-4,4′-diaminodiphenyl ether. *Polym J* 2011; **43**(10): 866–868.
15. Bowles KJ, Papadopoulos DS, Inghram LL, et al. Longtime Durability of PMR-15 Matrix at 204 260 288 and 316 C. NASA/TM 2001-210602.
16. Thompkins SS. *Effect of thermal cycling on composite materials for space structures*. Hampton, VA: NASA Langley Research Center. pp 447–470.
17. Varna J, Joffe R, Berglund LA, et al. Effect of voids on failure mechanism in RTM laminates. *Compos Sci Technol* 1995; **53**: 231–249.
18. Akay M, Spratt GR and Meenan B. The effects of long-term exposure to high temperatures on the ILSS and impact performance of carbon fibre reinforced bismaleimide. *Compos Sci Technol* 2003; **63**(7): 1053–1059.